D'Archivio and Wickstead, https://doi.org/10.1083/jcb.201608043

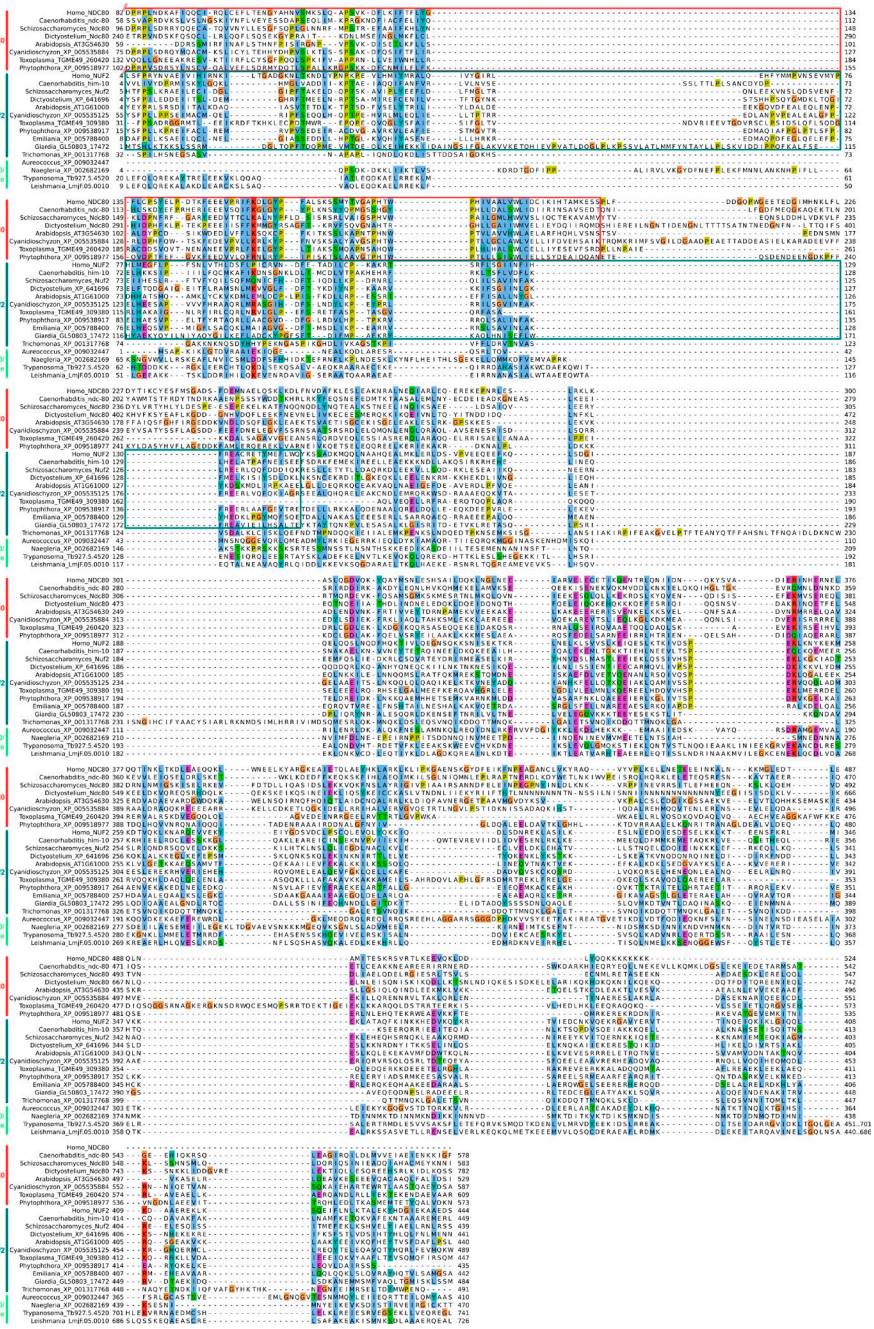

Figure S1. **Alignment of Ndc80- and Nuf2-like sequences from various eukaryotic models.** Boxes indicate the extent of the Pfam Ndc80_HEC1 (red) and Nuf2 (teal) domains. Excision of a section of ~250 aa present toward the C terminus of kinetoplastid sequences only (*Trypanosoma* and *Leishmania*) is indicated in the indices on the right.

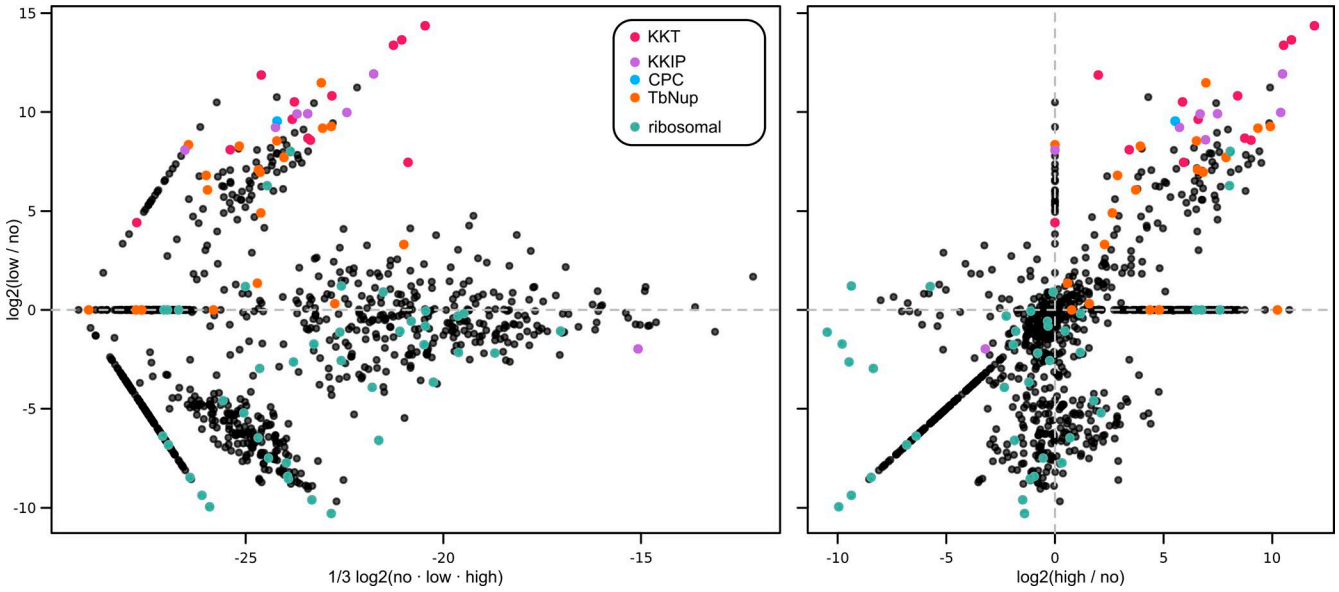

Figure S2. **Label-free semiquantitative proteomic data (Fig. 4) highlighting sequences from specific protein sets.** Highlighted are components of: KKT (Akiyoshi and Gull, 2014) and KKIP kinetochore sets, chromosome passenger complex (CPC; only TbAUK1 detected; Li et al., 2009), trypanosomal nucleoporins (TbNup; 19 out of 27 identified TbNups detected in any sample; DeGrasse et al., 2009; Obado et al., 2016), and proteins annotated as "ribosomal" in *T. brucei* TREU927 genome (TriTrypDB.org release 9.0 annotations; 62 out of 134 detected in any sample). For display, intensities of proteins not detected for a specific condition are set to an arbitrary minimum value.

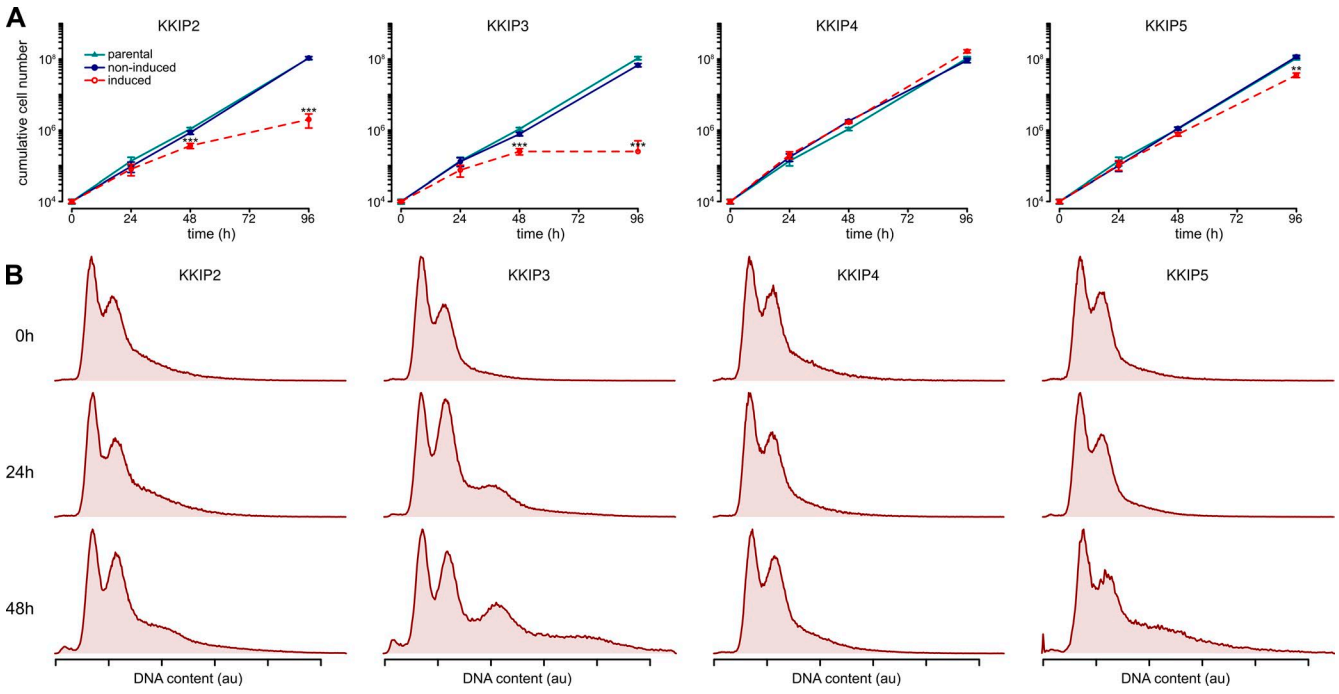

Figure S3. **Effect of depletion of KKIP2-5 by induction of RNAi.** (A) Growth of cells depleted of KKIP2, 3, 4, or 5. Error bars show SEM (n = 3; **, P < 0.01; ***, P < 0.001; Student's t test). (B) DNA content in RNAi-induced cells. Content was assessed by flow cytometry using fluorescence of propidium iodide stain (arbitrary units [au]). Representative data from two repeats shown.

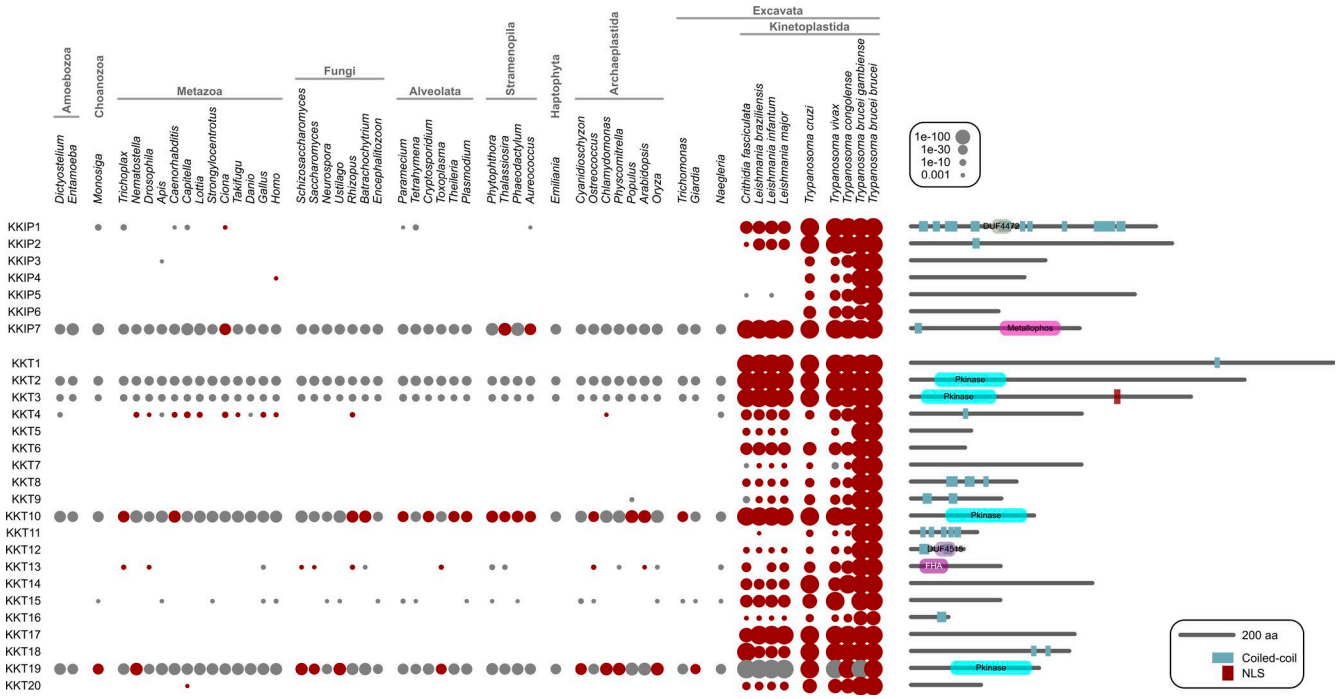

Figure S4. **BLAST-based similarity searches to show the distribution of easily detected orthologues to trypanosomal kinetochore proteins (KKT and KKIP) in the predicted proteomes of other Kinetoplastida and a wide range of eukaryotic lines.** Spot size represents the strength of BLAST hit (e-value). Red shows reciprocal best-BLAST hits between genomes; gray shows nonreciprocating hits. Predicted protein architectures: Pfam domains with e-value ≤ 0.001, regions of coiled-coil (Lupas et al., 1991), and predicted nuclear localization signals (NLStradamus) are shown for the *T. brucei* sequences.

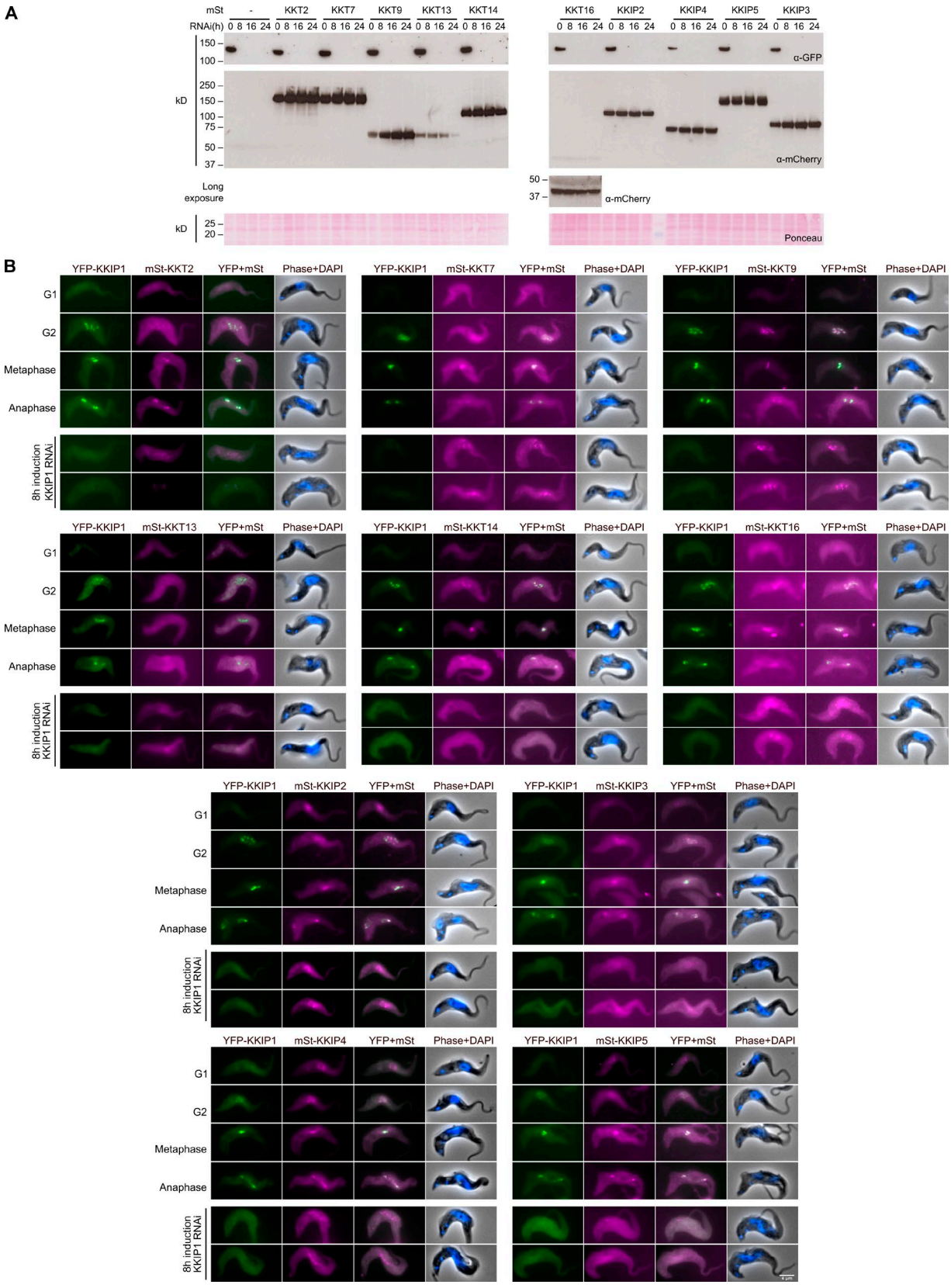

Figure S5. **Dependency of KKT and KKIP protein localization on KKIP1.** (A) Change in overall cellular levels of KKT and KKIP components upon depletion of KKIP1. Immunoblots are shown for cells expressing YFP-KKIP1 and mStrawberry-tagged KKT or KKIP protein. A long exposure of the blot is shown for mSt-KKT16. Protein loading is shown by Ponceau S stain. (B) Localization of KKT and KKIP components through the cell cycle and in cells depleted of KKIP1. Micrographs show bloodstream-form cells expressing YFP-KKIP1 and mStrawberry (mSt)-tagged KKT or KKIP protein. RNAi against *KKIP1* was induced for 8 h. mSt-KKIP2 remains in the nucleus on RNAi, but does not form kinetochore-like foci.

Table S1. **Top hits between kinetoplastid orthologue groups and an HMM of diverse Ndc80 and Nuf2 sequences**

Orthologue group	e-value	Score	*T. brucei* TREU927 gene identification numbers	Description (TriTrypDB)	Comment	PMID
OG5_141718	2.1×10^{-8}	71.8	Tb05.5K5.160; Tb927.5.4520	Hypothetical protein, conserved		
OG5_147717	2.4×10^{-8}	71.2	Tb11.v5.0753; Tb927.10.840	Hypothetical protein, conserved	FAZ6, localized to the FAZ	25736289
OG5_147082	5×10^{-8}	70.8	Tb927.2.4810	Hypothetical protein, conserved	TbCMF5	17227795
OG5_148374	9.9×10^{-8}	64.1	Tb927.11.4400	Hypothetical protein, conserved		
OG5_145178	1.3×10^{-7}	73	Tb927.10.1450	Plectin, putative		23264645
OG5_148122	1.8×10^{-7}	64	Tb927.6.4550	Hypothetical protein, conserved		
OG5_144798	2.1×10^{-7}	65.8	Tb927.8.780	Hypothetical protein, conserved		
OG5_131340	2.3×10^{-7}	64	Tb927.4.2140	MBO2, flagellar component		17227795
OG5_148036	3.6×10^{-7}	65.1	Tb927.9.1600	Hypothetical protein, conserved		
OG5_130053	4.1×10^{-7}	59.1	Tb927.11.16090	Outer dynein arm docking complex, putative (DC2)		20126266
OG5_148971	5.3×10^{-7}	61.4	Tb927.10.4200	Hypothetical protein, conserved		
OG5_127071	8.8×10^{-7}	60.8	Tb927.11.13920; Tb927.3.2040; Tb927.5.2090	Kinesin, putative	OG contains Kinesin-2 and Kinesin-17 members	

Table S2. **KKIP1-interacting proteins and controls localized in trypanosomes**

Gene identification number	Name	Localization	Identical polypeptide	Indistinguishable by MS	Description (TriTrypDB)
Test set					
Tb927.5.4520	KKIP1	Kinetochore	Tb05.5K5.160		Hypothetical protein, conserved
Tb927.5.1320	KKIP2	Kinetochore			Hypothetical protein, conserved
Tb927.10.6700	KKIP3	Kinetochore			Hypothetical protein, conserved
Tb927.7.3080	KKIP4	Kinetochore			Hypothetical protein, conserved
Tb927.7.6630	KKIP5	Kinetochore			Hypothetical protein, conserved
Tb927.1.4680	KKIP6	Kinetochore			Hypothetical protein, conserved
Tb927.11.12480	KKIP7	Kinetochore			Kinetoplastid-specific phosphoprotein phosphatase, putative
Tb927.3.3740		Nuclear			Hypothetical protein, conserved
Tb927.9.13970		Nuclear			Hypothetical protein, conserved
Tb927.9.1410		Nuclear			Hypothetical protein, conserved
Tb927.11.3710		Flagellar			Hypothetical protein, conserved
Tb927.10.14500		Not localized			Hypothetical protein, conserved
Tb927.11.9510		Nuclear periphery			Nucleic acid binding protein, putative
Low cross-link controls					
Tb927.9.10100		Cytoplasmic			Hypothetical protein, conserved
Tb927.5.1900		Not localized			Hypothetical protein, conserved
Tb927.7.4910		Flagellar	Tb11.v5.0172		Hypothetical protein, conserved
Tb927.8.4950		Cytoplasmic			Kinesin, putative
Tb927.9.10400		Nucleolar			Hypothetical protein, conserved
High cross-link controls					
Tb927.10.14630		Nucleolar		Tb927.10.14750	Fibrillarin, putative
Tb927.11.5230		Nuclear			Hypothetical protein, conserved
Tb927.11.12380		Nuclear			Hypothetical protein, conserved

Provided online are two Excel tables. Table S3 provides data from label-free semiquantitative mass spectrometry of KKIP1-interacting proteins. Table S4 shows primer sequences used in the generation of constructs for endogenous locus tagging and RNA interference.

References

Akiyoshi, B., and K. Gull. 2014. Discovery of unconventional kinetochores in kinetoplastids. *Cell.* 156:1247–1258. http://dx.doi.org/10.1016/j.cell.2014.01.049

DeGrasse, J.A., K.N. DuBois, D. Devos, T.N. Siegel, A. Sali, M.C. Field, M.P. Rout, and B.T. Chait. 2009. Evidence for a shared nuclear pore complex architecture that is conserved from the last common eukaryotic ancestor. *Mol. Cell. Proteomics.* 8:2119–2130. http://dx.doi.org/10.1074/mcp.M900038-MCP200

Li, Z., T. Umeyama, and C.C. Wang. 2009. The Aurora Kinase in *Trypanosoma brucei* plays distinctive roles in metaphase-anaphase transition and cytokinetic initiation. *PLoS Pathog.* 5:e1000575. http://dx.doi.org/10.1371/journal.ppat.1000575

Lupas, A., M. Van Dyke, and J. Stock. 1991. Predicting coiled coils from protein sequences. *Science*. 252:1162–1164. http://dx.doi.org/10.1126/science.252.5009.1162

Obado, S.O., M. Brillantes, K. Uryu, W. Zhang, N.E. Ketaren, B.T. Chait, M.C. Field, and M.P. Rout. 2016. Interactome mapping reveals the evolutionary history of the nuclear pore complex. *PLoS Biol.* 14:e1002365. http://dx.doi.org/10.1371/journal.pbio.1002365